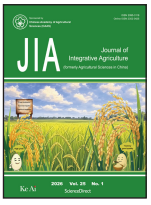
Journal of Integrative Agriculture 2026, 25(1): 138–149

Available online at ScienceDirect

Journal of Integrative Agriculture



RESEARCH ARTICLE

Insights into the geranylgeranyl pyrophosphate synthase (GGPPS) gene family in *Osmanthus fragrans* and the role of *OfGGPPS13* in the formation of floral color and aroma

Hanruo Qiu, Qingyin Tian, Guimin Zeng, Chenchen Xie, Xiulian Yang, Lianggui Wang, Yuanzheng Yue#

State Key Laboratory of Tree Genetics and Breeding/Collaborative Innovation Center of Sustainable Forestry in Southern China of Jiangsu Province/ College of Landscape Architecture/College of Forestry and Grassland & Soil and Water Conservation, Nanjing Forestry University, Nanjing 210095, China

Highlights

- Genome-wide identification of 24 *OfGGPPS* genes reveals a key flower preferentially expressed enzyme gene, *OfGGPPS13*.
- *OfGGPPS13* diverts metabolic flux to enhance *β*-carotene synthesis but reduces scent volatiles.

Abstract

Osmanthus fragrans is most famous for its strong aroma, and different varieties have different degrees of fragrance and color. Fragrance and color are important factors affecting the ornamental quality of *O. fragrans*. Terpenoids are important secondary metabolites in plants, with *β*-carotene (C40) being the major pigment substance and linalool (C10) being the key aromatic component in *O. fragrans*. The geranylgeranyl pyrophosphate synthase genes (*GGPPS*s) play important roles in secondary metabolism in plants. However, the functions of the GGPPS family in floral color and fragrance formation has rarely been reported in *O. fragrans*. In this study, 24 *OfGGPPS* genes were identified and classified into two subfamilies. The *OfGGPPSs* showed tissue-specific expression and *OfGGPPS13* had highest expression in flowers. The OfGGPPS13 protein was localized to chloroplasts. The transcriptome data of *OfGGPPS13* was verified by qRT-PCR and the expression level in 'Wanyingui' with strong aroma was higher than that in 'Zhuangyuanhong' with deep color at different flower development stages. Transient overexpression of *OfGGPPS13* in *O. fragrans* petals showed that *OfGGPPS13* increased the *β*-carotene content, the main color substance of *O. fragrans*, but decreased the linalool content, the main volatile organic compound (VOC) in the floral aroma of *O. fragrans*. *OfGGPPS13* was indicated as the critical gene related to terpenoid synthesis in the floral aroma and color formation in *O. fragrans*. Our findings provide gene resources on the GGPPS gene family for further revealing the molecular regulation mechanism of the floral color and aroma formation in *O. fragrans*.

Keywords: GGPPS gene family, *Osmanthus fragrans*, floral color and aroma formation, functional characterization

1. Introduction

Osmanthus fragrans, known as one of the top ten famous flowers in China, has multiple uses, such as ornamental, edible, and flavoring additive uses. Based on color and flowering period, *O. fragrans* is usually divided into four species groups: Asiaticus, Albus, Luteus and Aurantiacus, and there are two extreme varieties: Albus Group with strong aroma and lighter color and Aurantiacus Group with darker color and lighter aroma. However, in the different cultivars, the characteristic aromas come from the complex combinations of terpenes. Among them, linalool contributes significantly to volatiles responsible for the fragrance in *O. fragrans* (Cai *et al.* 2014). In addition to the above volatile terpene metabolites, there are also nonvolatile terpenoid metabolites that confer color to plants, such as carotenoids and chlorophyll. (Pichersky and Gershenzon 2002).

Terpenoids are compounds based on isoprene (C5) as the basic unit and their derivatives, with a wide range of classifications and types, and they are produced by a series of polymerization chain reactions of isopentenyl diphosphate

Received 7 June 2024; Received in revised form 13 December 2024; Accepted 29 April 2025; Available online 17 November 2025
#Correspondence Yuanzheng Yue, E-mail: yueyuanzheng@njfu.edu.cn

© 2026 CAAS. Publishing services by Elsevier B.V. on behalf of KeAi Communications Co. Ltd. This is an open access article under the CC BY-NC-ND license (http://creativecommons.org/licenses/by-nc-nd/4.0/). Peer review under responsibility of Editorial Board of *Journal of Integrative Agriculture*.
doi: 10.1016/j.jia.2025.11.029

(IPP) and its isomer dimethylallyl diphosphate (DMAPP) (Mcgarvey and Croteau 1995). There are two pathways in plants that can synthesize terpenoids: the mevalonate (MVA) pathway and the 2-C-methyl-D-erythritol-4-phosphate (MEP) pathway (Newman and Chappell 1999). The MEP pathway mainly synthesizes geranyl pyrophosphate (GPP) and geranylgeranyl pyrophosphate (GGPP), which are located in the plastids. GPP is the precursor of monoterpenes (C10), while GGPP is used for the biosynthesis of di- (C20), tetra- (C40), and polyterpenes (Cn) (Simkin *et al.* 2011). The generation and modification of terpenoids, including oxidation-reduction, acylation, and glycosylation reactions, leads to the structural diversity of terpenes (Barja and Rodriguez-Concepcion 2021). Most essential plant isoprenoids use GPP and GGPP as precursors, whose pools are important branching points in isoprene synthesis (Vranova *et al.* 2011). The terpenoid synthesis is regulated by multiple enzymes in plants. GGPP can act as the precursor substrate for both nonvolatile terpenoids and volatile terpenoids, which are catalyzed by GGPPS (Beck *et al.* 2013; Yan *et al.* 2023). GGPPS proteins contain two aspartate-rich motifs, FARM and SARM (DDxxxxD and DDxxD; x is any amino acid), which chelate with Mg^{2+} to participate in the binding of substrates, and are essential for GGPP biosynthesis, thereby affecting the catalytic activity of GGPPS (Liang *et al.* 2002; Liang 2009).

Two types of GGPPS, large subunits (LSUs) and non-active small subunits (SSUs), have been discovered in plants. Both FARM and SARM domains can be found in LSUs, while SSUs lack at least one and contain at least a “CxxxC” motif (Chen Q *et al.* 2015). SSUs are catalytically inactive on their own and cannot catalyze reactions through the formation of homodimers (Barja and Rodriguez-Concepcion 2021). There are two types of SSUs in plants. SSUIs are related to the production of GPP and monoterpenes, which are mainly found in flowering plants, whereas the interaction of SSUIIs with LSUs can produce GPP and simultaneously enhance the production of GGPP (Wang and Dixon 2009). In *Antirrhinum majus*, GGPPS.SSU, which is inactive alone, can form a heterodimer with GGPPS.LSU *in vivo* to modulate its activity (Tholl *et al.* 2004). In *Humulus lupulus*, GGPPS.SSU forms a heterodimer with GGPPS.LSU to produce GPP and GGPP, and the enzyme activity of the heterodimer is significantly higher than the catalytic efficiency of GGPPS.LSU itself (Wang and Dixon 2009). NtGGPPS.LSU can form the homodimer and catalyze the synthesis of GGPP in *Nicotiana tabacum*, but the content of monoterpenes increases in transgenic tobacco after binding with AmGGPPS.SSUI (Orlova *et al.* 2009). The GGPPS proteins in different subfamilies may have different expression levels in each tissue and be located in different subcellular compartments of the same plant (Okada *et al.* 2000; Huang *et al.* 2019). A total of 12 GGPPS proteins have been found in *Arabidopsis thaliana*, which are expressed highest in roots, leaves, stems, and flowers and are localized in the chloroplast, mitochondria, or endoplasmic reticulum with different functions for plant development (Okada *et al.* 2000).

GGPP, which is synthesized by *GGPPSs*, is an important precursor of the carotenoid metabolic pathway, and its production directly affects the synthesis of downstream carotenoids (Lois *et al.* 2000; Matthews and Wurtzel 2000). The *LtuGGPPS2* gene had the highest expression in the flowers of *Liriodendron chinense*, and its expression level during petal development was consistent with changes in the terpenoid content in petals. After heterologous overexpression of *LuGGPPS2* in *A. thaliana*, the carotenoid content of transgenic plants increased by 44.42% (Zhang *et al.* 2021). The overexpression of the designed mutant gene d-NtGGPPS1 in *N. tabacum* resulted in consistent results for transient and stable expression, with increased levels of carotenoids in leaves (Dong *et al.* 2022). These results indicate that *GGPPSs* can promote carotenoid biosynthesis and may be responsible for plant coloration.

Spatiotemporal variations in the expression of *GGPPSs* show a high degree of consistency with the synthesis and release patterns of plant aroma substances. The expression abundance of *GGPPSs*, which are key enzyme genes, contributes to differences in aroma content among plant varieties, and their expression patterns are related to the release of floral aroma substances. In different *Syringa* varieties, the expression levels of *GGPPSs* were positively correlated with the contents of floral aroma substances. Compared with the light fragrance variety *S. oblata*, the concentrated fragrance variety *S. vulgaris* had a higher expression level of *GGPPSs*. The differential expression of *GGPPSs* between the two varieties led to differences in floral content, suggesting that they might be key genes promoting the synthesis of volatile metabolites in lilac (Yang *et al.* 2023).

In addition, the spatial and temporal differential expression of *GGPPSs* in plants affect the release of plant aroma compounds. For example, *Rosa damascena* is an important fragrant flower in the perfume industry. The content of aroma compounds in flowers increases during flower development, reaches its peak in the blooming stage, and decreases during flower senescence, which is consistent with the expression trend of *RdGGPPSs*. It has been speculated that the accumulation of aroma substances in the flowers of *R. damascena* may be related to the expression of *GGPPSs*, and *GGPPSs* may play important roles in regulating the aromatic components in *R. damascena* (Rasouli *et al.* 2018). IPP and DMAPP are common precursors for the synthesis of GPP, GGPP, and FPP (farnesyl pyrophosphate). By adjusting the ratio between IPP and DMAPP concentrations, the catalytic products of GGPPS can be altered, thereby affecting the synthesis of plant aroma compounds. As in *Capsicum annuum*, higher DMAPP concentrations led to the production of large amounts of GPP catalyzed by CaGGPPS (Bouvier *et al.* 2000). The functions of *GGPPSs* have been reported in other plants, but little is known about the formation of floral color and fragrance in *O. fragrans*.

In this study, the number of GGPPS family members was identified using bioinformatics techniques based on the whole genome sequences of *O. fragrans*. According to the expression patterns in two different *O. fragrans* varieties, we selected the *OfGGPPS13* gene to perform functional analysis to reveal its function in *O. fragrans* monoterpene and carotenoid biosynthesis. This work will provide valuable GGPPS family

gene resources for deeper investigation of the molecular regulation mechanism of floral color and aroma in *O. fragrans*.

2. Materials and methods

2.1. Plant materials

Osmanthus fragrans trees were grown in the fields of Nanjing Forestry University, Nanjing, China. Flowers of 'Zhuangyuanhong' and 'Wanyingui' were collected at five stages (S1–S5: bud-pedicel stage, bud-eye stage, primary blooming stage, full blooming stage, and flower fading stage) from 9:00 to 11:00, and then cryopreserved. Fresh flowers of *O. fragrans* at S4 were collected from 9:00 to 16:00 and then used for transient transformation. The flowers were sampled on the sunny days to avoid the weather effect on the flower fragrance. One gram of randomly picked petal tissue was considered one replicate. *Nicotiana tabacum* plants were cultivated in a glass greenhouse at Nanjing Forestry University. Three biological replicates were set up for each experiment.

2.2. Bioinformatics analysis of the GGPPS family in *O. fragrans*

Multiple GGPPS protein sequences (Appendix A) were downloaded from the *Arabidopsis thaliana* database, the *Oryza sativa* Data Center, the Solanaceae database, the NCBI database, and the UniProt Protein Sequence database. The full-length amino acid sequences of the *A. thaliana* protein family were used as a probe to compare with the *O. fragrans* genome database (Yang *et al.* 2019) using TBtools software. The TBtools alignment results were then subjected to bidirectional Blast alignment in the NCBI database to obtain potential members. Based on the conserved structural domains of NCBI CDD, we selected candidate members in the *O. fragrans* GGPPS gene family. The physical and chemical properties of OfGGPPS proteins were analyzed using Expasy online analysis software and ProtScale software. The subcellular localization of GGPPS proteins in *O. fragrans* was predicted using WoLF PSORT, BaCelLo, and Plant-Ploc online websites. Multiple sequence comparison analysis was performed on 181 GGPPS amino acid sequences from various plant species using MEGA11 software, and a phylogenetic tree was constructed using MEGA11 (neighbor joining, NJ) and then visualized and analyzed using iTOL (https://itol.embl.de/).

The gene structure information of *OfGGPPSs* was extracted from the annotation file of the *O. fragrans* genome. The identified OfGGPPS protein sequences were submitted to the online website MEME for motif analysis. The phylogeny, motif, and gene structure of *OfGGPPSs* were visualized using TBtools software, and multiple sequence alignment of OfGGPPSs was performed using MEGA11 and Jalview software. TBtools was used to map the distribution of *OfGGPPSs* on chromosomes. The McScanx method was used to classify the replication methods of *OfGGPPSs* into tandem and segmental replications, and the data were visualized using the TBtools toolkit. All website URLs are included in Appendix B.

2.3. Expression pattern analysis of the GGPPS family in *O. fragrans*

In our previous study, we have obtained the transcriptomic data of the different tissues in 'Rixianggui' in Asiaticus Group (Yang *et al.* 2019), hence, we used these data to analyze the expression patterns of *OfGGPPSs* in different tissues. 'Wanyingui' in Albus Group and 'Zhuangyuanhong' in Aurantiacus Group are two extreme varieties in the comparison of floral aroma and color, so we chose them for comparative analysis to identify key genes involved in the floral aroma and color formation. The unpublished transcriptome sequencing of *O. fragrans* was performed using the Illumina HighSeqTM2000 sequencing platform, and the plant materials used were three varieties of *Osmanthus*, namely 'Rixianggui', 'Wanyingui', and 'Zhuangyuanhong'. The different tissues used for transcriptome sequencing were roots, stems, leaves (young and mature), and flowers (S4) of 'Rixianggui'. For transcriptome sequencing, the petals of 'Wanyingui' and 'Zhuangyuanhong' collected at five stages were used. Based on the transcriptome data, fragments per kilobase of exon model per million mapped fragments (FPKM) values of *OfGGPPS* family members extracted from the *O. fragrans* transcriptome database for different tissues and different species were visualized using TBtools. The differential expression were determined by a fold change≥2 and a *P*-value<0.05.

2.4. Subcellular localization of the OfGGPPS13 protein

The full-length coding sequence (CDS) of *OfGGPPS13* was extracted from the *O. fragrans* genome file. The cleavage sites were analyzed using BioXM software, and the common cleavage sites (5′SmaI-3′KpnI) that were not present in the target gene but in the vector were selected. The amplification primers were designed using CE Design software (Appendix C), so that the CDS of *OfGGPPS13* was obtained. We used the flower cDNA of 'Rixianggui', 'Wanyingui', and 'Zhuangyuanhong' as the templates for *OfGGPPS13* amplification. The blasting results of these sequences showed that the different sites were not in the conserved functional domains of OfGGPPS13 (Appendix D). Therefore, we randomly chose the 'Rixianggui' as the template for the next functional verification of *OfGGPPS13*. The published methods were used for vector construction and transformation (Ding *et al.* 2020). 35s::GFP–*OfGGPPS13* and empty pSuper1300-GFP were introduced into the tobacco leaves using *Agrobacterium*-mediated transformation (GV3101). The GFP fluorescence signal was monitored under the LSM710 confocal microscopy (ZEISS, Jena, Germany) 48 h after transformation (20°C with a 15-h photoperiod).

2.5. Transient overexpression of *OfGGPPS13* in *O. fragrans* petals

The pSuper1300-GFP vector inserted with the *OfGGPPS13* coding region was transformed into GV3101 using a published method (Han *et al.* 2016). Using the method for transient overexpression in *O. fragrans* petals previously published by our research group (Liu *et al.* 2022), the S4 petals of *O. fragrans* var. leteus were vacuum infiltrated with

Agrobacterium and then transferred to 0.5% agar medium in the dark for 48 h. At S4 stage, the *O. fragrans* petals are nearly spreading, the flower color turns dark, and the flower fragrance is strong. After 48 h in the dark, the flower status of the control group (empty vector) and the experimental group was similar.

2.6. Quantitative real-time PCR (qRT-PCR) analysis

The petals of 'Wanyingui' and 'Zhuangyuanhong' at five stages and the transient overexpression petals were collected. Total RNA was isolated using a RNAprep Pure Plant Kit (Tiangen, Beijing, China). Complementary DNA (cDNA) was synthesized by One-Step gDNA Removal and cDNA Synthesis Super Mix (Transgen, Beijing, China). The specific primers of *OfGGPPS13*, *OfCCD4*, and *OfTPS1a/1b* were designed by Primer Premier 5.0. *OfRAN* was used as a normalizer (Appendix E). Each qRT-PCR assay was performed on Step One Plus real-time PCR (Thermo Fisher Scientific Inc., Massachusetts, USA), containing three biological samples, with three technical replicates per biological sample.

2.7. Analysis of aroma components of *OfGGPPS13* transgenic petals

Headspace solid-phase microextraction (SPME) was used to collect the volatile components. A 0.6 g transgenic petal sample was placed in a 20 mL glass vial as a biological replicate, with 3 μL of methyl laurate diluted 3,000-fold with methanol (Macklin Inc., Shanghai, China) added as the internal standard. The SPME fiber of DB-5 MS (Supelco Inc., Bellefonte, USA) was used for extraction and desorption using a published method (Liu *et al.* 2022). The desorbed aroma compounds were identified using Trace DSQ gas chromatography-mass spectrometry (GC-MS) equipment (Ji 2021).

2.8. Determination and analysis of products on the MEP pathway in *OfGGPPS13* transgenic petals

Three biological replicates with three technical replicates each were set up using *O. fragrans* petals transfected with the empty vector of pSuper1300 as the control. The contents of GGPP, GPP, and *β*-carotene in *OfGGPPS13*-overexpressing petals were determined according to the instructions of the Plant GGPP, GPP, and *β*-carotene enzyme-linked immunosorbent assay (ELISA) kits (Huding Biology, Shanghai, China), respectively. The GGPPS content in *OfGGPPS13*-overexpressing petals was determined according to the the instructions of the Plant GGPPS and GPPS Substrate Competition Assay Kit (Huding Biology).

2.9. Statistical analysis

All data were analyzed with Student's *t*-test or least significant difference (LSD) test using SPSS Statistics 22 software and SIMAC software (*, $P<0.05$; **, $P<0.01$; ***, $P<0.001$). The values are the means±standard error (SE; $n\geq3$).

3. Results

3.1. Identification of *OfGGPPSs*

In total, 24 putative *GGPPSs* were identified from the *O. fragrans* genome based on conservative domain screening. According to their chromosomal locations, these genes were named *OfGGPPS1–OfGGPPS24*. The lengths of the OfGGPPS proteins were between 179 (OfGGPPS1) and 422 (OfGGPPS23) aa, and the corresponding molecular weights ranged from 19,590.77 (OfGGPPS1) to 46,813.83 (OfGGPPS23) kDa. The isoelectric points ranged from 5.07 to 8.19, and the majority of OfGGPPSs were acidic proteins (isoelectric point<7), except for OfGGPPS22 (isoelectric point>7). The instability index ranged from 31.78 to 59.23, among which 15 proteins were unstable proteins (instability index>40) and 9 proteins were stable proteins (instability index<40). The aliphatic index ranged from 80.38 to 102.7 (Appendix F).

Subcellular localization of the 24 members in *O. fragrans* was predicted using the WoLF PSORT, BaCelLo, and Plant-Ploc online websites (Appendix G). The results showed that most of the predictions from the three websites were consistent, and the predicted localizations of OfGGPPS2/5/6/10/11/12/13/14/18/21/23 were all in the chloroplast. All 24 OfGGPPS proteins had clear hydrophilic and hydrophobic regions, among which OfGGPPS17, OfGGPPS19, and OfGGPPS20 had fewer hydrophilic regions than hydrophobic regions, indicating that they are hydrophobic proteins. There were more remaining hydrophilic regions of the OfGGPPS polypeptide chains than hydrophobic regions, indicating hydrophilic proteins. The peptide chains of the remaining OfGGPPSs had more hydrophilic regions than hydrophobic regions, indicating that they were hydrophilic proteins (Appendix H).

3.2. Phylogenetic analysis of *OfGGPPSs*

The evolutionary relationships of *O. fragrans* GGPPS proteins were investigated, and 181 protein sequences from 60 species were used to construct a phylogenetic tree. The 181 GGPPS proteins were divided into 5 subfamilies named sub1–5, which contained 3, 4, 13, 25, and 136 GGPPSs (Fig. 1). Of these, sub5 had the highest number of GGPPS protein members, including 17 OfGGPPSs, 10 AtGGPPSs, 7 PtGGPPSs, and 3 SlGGPPSs. Sub4 contained the remaining 7 OfGGPPSs and SSUs identified from different species. The GGPPS proteins in sub3 were mostly found in gymnosperms. Sub2 and sub1 contained only the GGPPS proteins from 1 bryophyte specie and 3 algae species, respectively. Overall, the number of *GGPPSs* increased with species evolution. OfGGPPSs were only concentrated in sub4 and sub5.

3.3. Chromosomal location and gene duplication of *OfGGPPSs*

OfGGPPSs are distributed on 13 chromosomes, and there were three *GGPPS*s on Chr19. Compared with Chr19, Chr01 with the longest chromosome length had two *GGPPS*s, while Chr23 with the shortest chromosome length only had one *GGPPS* gene (Fig. 2-A). Overall, there was no correlation between the number of *GGPPS*s present on chromosomes and chromosome length.

There were no tandem duplication events in the *GGPPS* genes of *O. fragrans*. The MCScanX method

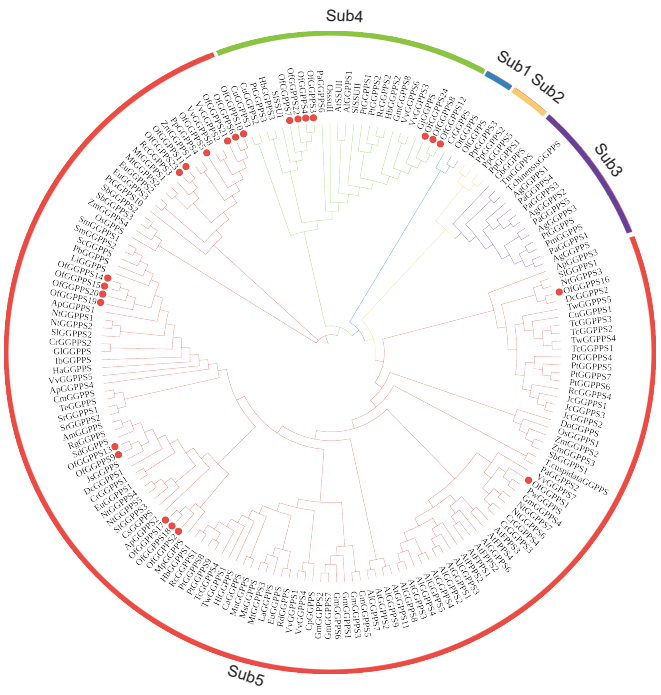


Fig. 1 Phylogenetic tree of GGPPS proteins. The phylogenetic tree was generated with MEGA 11 software using the neighbor-joining method. OfGGPPSs are marked by red cycles.

was used to compare and obtain 22 genes with fragment duplication events. These results indicated that a part of *OfGGPPS*s may be generated by gene fragment duplication which may be crucial for the amplification of *OfGGPPSs* (Fig. 2-B).

3.4. Gene structure of *OfGGPPSs*

The 24 *OfGGPPSs* contained 1–12 exons, of which *OfGGPPS11* and *OfGGPPS23* had the most exons (12). The gene with the most introns had 11 introns, and the least had none (Fig. 3-C). The *OfGGPPSs* encoding adjacent proteins in the phylogenetic tree had the same or similar exon–intron structures (Fig. 3-A and C).

There were 10 conserved motifs (motifs 1–10) found in 24 OfGGPPS proteins (Fig. 3-B and D). Most members of adjacent branches of the phylogenetic tree exhibited similar motif organizations. Motif 7 existed in all OfGGPPSs, and motif 10 was only present in sub4. Motifs 2/3/4/5/7 were found in the OfGGPPSs of sub4, and motifs 1/2/4/7 were found in the OfGGPPSs of sub5. Generally, the motif composition and location of OfGGPPSs in each subfamily were essentially the same, which demonstrated that the OfGGPPSs in the same subfamily may play similar roles.

OfGGPPSs contained two conserved Asp-rich structural domains, FARM and SARM (Fig. 4), with a conserved sequence of DDxx(xx)D (where D is aspartic acid and x is any amino acid). These two domains were the active sites of the OfGGPPS enzyme. Some OfGGPPSs also had CxxxC structural domains (where x is any amino acid) that may interact with other proteins. In addition, there was a chain length-determining domain (CLD) located upstream of the first characteristic sequence FARM at the N-terminus of the OfGGPPSs, which determined the length of the catalytic product of the OfGGPPS protein (Satta *et al.* 2022).

There were 17 OfGGPPS proteins clustered with AtGGPPS1–4, AtGGPPS6–11, and RdGGPPSs (Fig. 1) that belonged to sub5. All 17 OfGGPPS proteins had the conserved domain “DDxx(xx)D” and belonged to LSU. The remaining 7

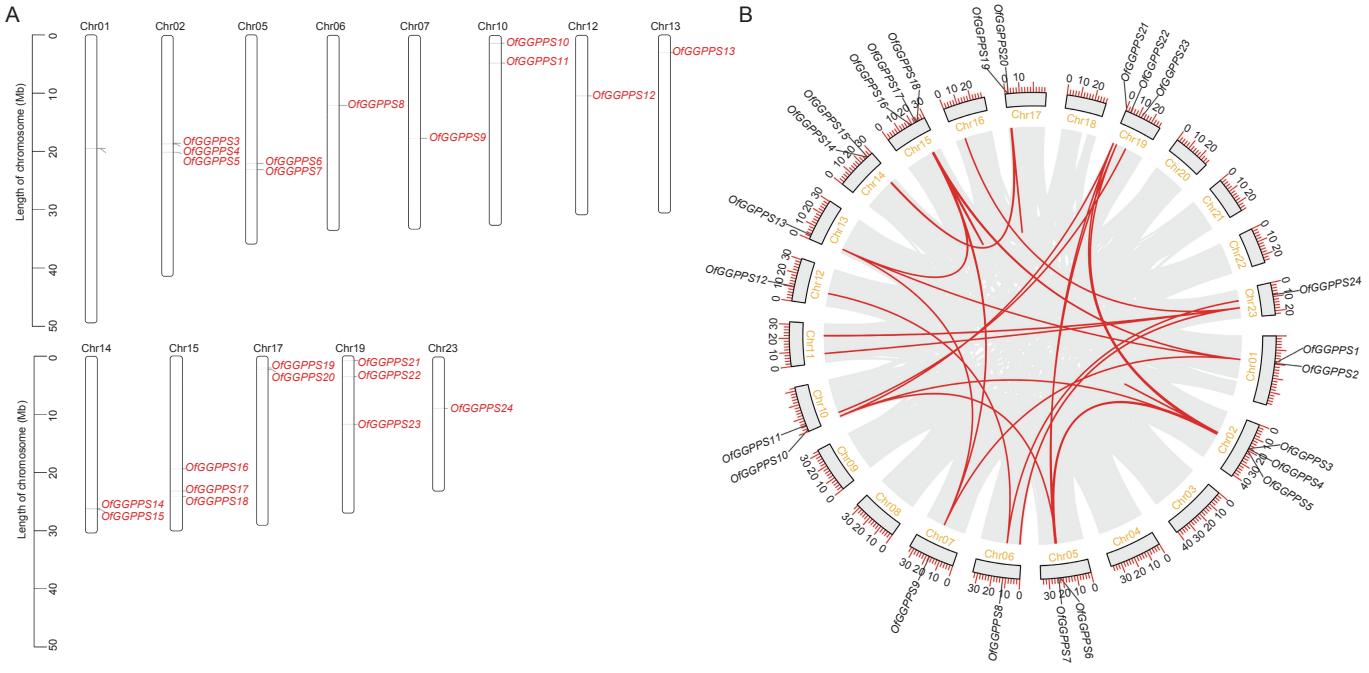


Fig. 2 Chromosomal distribution and gene duplication of *OfGGPPSs*. A, distribution of *OfGGPPSs* on chromosomes. B, synteny duplication of *OfGGPPSs*. All collinear blocks in the *Osmanthus fragrans* genome are indicated by gray lines, and the *OfGGPPSs* pairs of fragment replication events are represented by red lines.

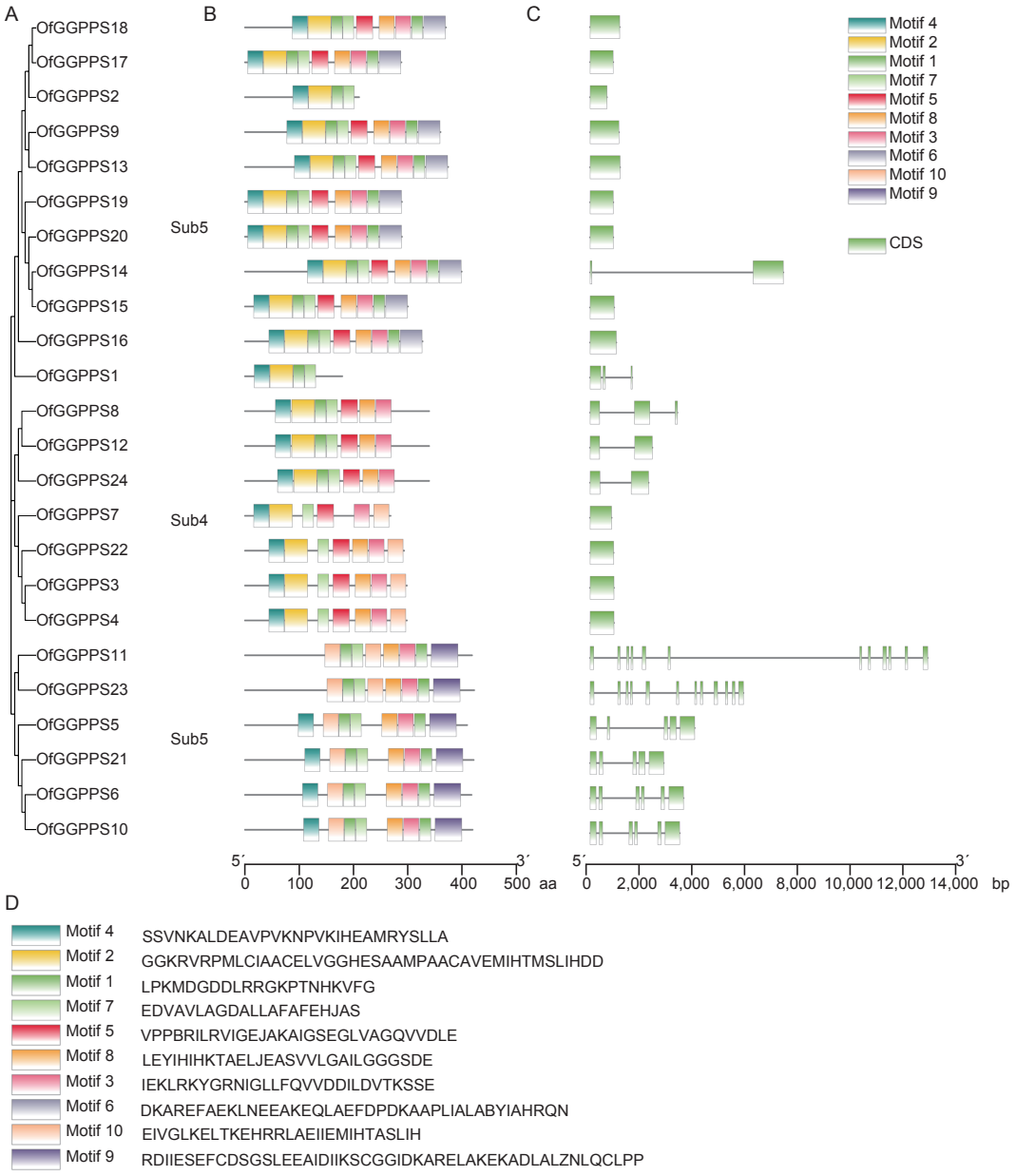


Fig. 3 The gene structure of *OfGGPPSs* were analyzed. A, phylogenetic tree of the *OfGGPPS* gene family. B, conserved motif amino acid distribution. C, gene structure analysis of *OfGGPPSs*. D, conserved motif amino acid.

OfGGPPS proteins clustered with AtGGPPS12 and belonged to sub4. Among them, OfGGPPS3/4/7/22 lacked two "DDxx(xx)D" conserved regions and contained a "CxxxC" motif. These four OfGGPPS proteins clustered with SlSSUI and belonged to SSUI. However, OfGGPPS8/12/24 clustered with AtSSUII, SlSSUII, and OsSSUII and had the first aspartic acid conserved motif, FARM, and the two "CxxxC" motifs.

The sequence structures of OfGGPPSs clustered together were relatively consistent with the gene structure. The reliability of the classification was further demonstrated by the similar gene structures and conserved motifs in each category.

3.5. Expression patterns of *OfGGPPSs* in different tissues

The FPKM values of 24 *OfGGPPSs* obtained from transcriptome data of different tissues of 'Rixianggui' were visualized using TBtools (Fig. 5-A). Three of the *OfGGPPS* genes (*OfGGPPS10/11/12*) were not found in this transcriptome data, while the remaining 21 *OfGGPPS* genes showed different expression patterns; among them, 18 *OfGGPPSs* were expressed in all 5 tissues except *OfGGPPS5/7/16*. Of the *OfGGPPSs*, 5, 7, and 9 had higher expression levels in roots, young leaves, and mature leaves, respectively. *OfGGPPS8/9/13/15/21/22* had significantly higher expression levels in flowers. Overall, the expression patterns of *OfGGPPSs* exhibited tissue specificity.

3.6. Expression patterns of *OfGGPPSs* in different cultivars

The FPKM values of the 24 *OfGGPPSs* were obtained from

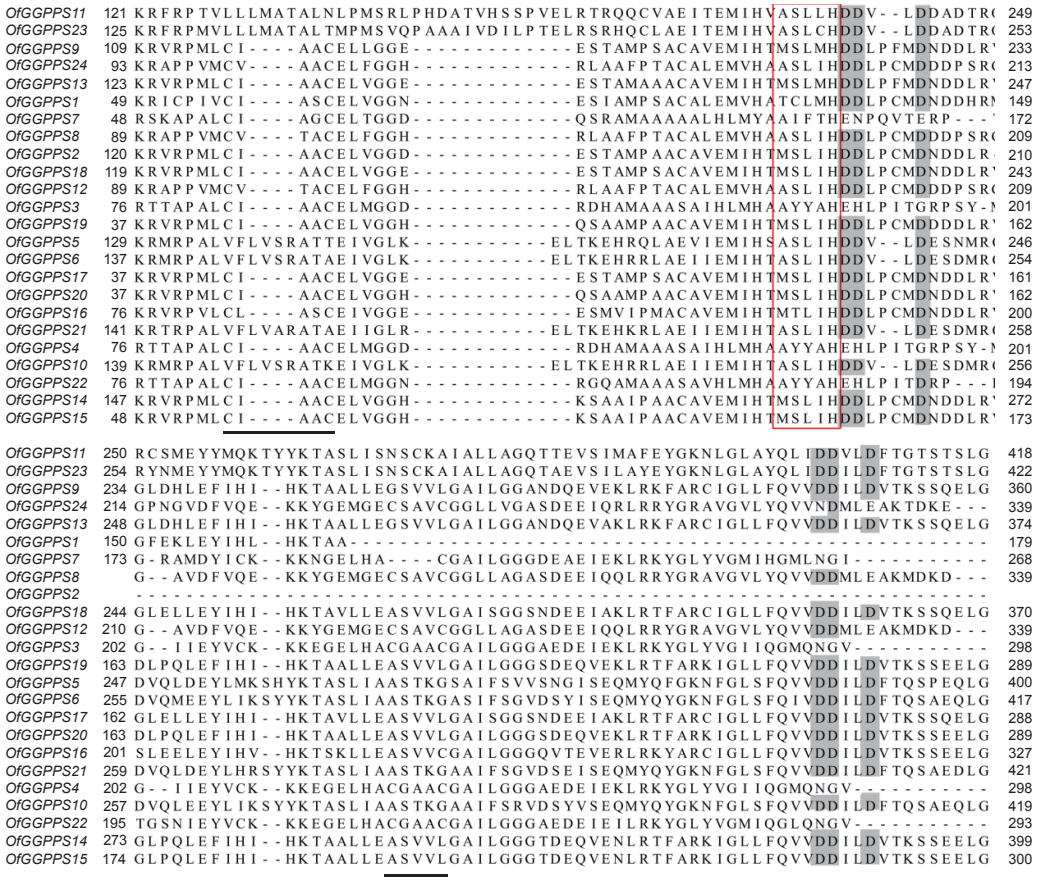


Fig. 4 Sequence alignment of conserved domains of OfGGPPSs. The two conserved aspartate-rich motifs DD(x2-4)D are highlighted in gray. The two CxxxC motifs are underlined in black. The chain length-determining CLD sites are marked with a red frame.

transcriptome data of 'Wanyingui' and 'Zhuangyuanhong', and visualized using TBtools (Fig. 5-B). Only *OfGGPPS5/7* were not expressed in both varieties, while the remaining 22 *OfGGPPS*s exhibited different expression patterns. Most of the *OfGGPPS*s expressed in 'Wanyingui' had higher expression levels during S2 and S3. The expression levels of the *OfGGPPS*s in 'Zhuangyuanhong' were relatively high from S2 to S4. However, the expression levels of most numbers in two cultivars were firstly increased and then decreased, which was consistent with the release pattern of floral fragrance. The expression levels of some *OfGGPPSs*, such as *OfGGPPS12* in 'Wanyingui', were higher than those in 'Zhuangyuanhong', which may be related to the aroma formation in *O. fragrans* flowers. The expression levels of some *OfGGPPSs*, such as *OfGGPPS13* in 'Zhuangyuanhong', was significantly higher than those in 'Wanyingui', suggesting that *OfGGPPS13* may be involved in color formation in *O. fragrans* flowers.

qRT-PCR validation was performed on *OfGGPPS13* to further investigate its potential function in the floral fragrance and color of *O. fragrans*. The results were correlated with the transcriptome FPKM values, and the transcriptome data of *OfGGPPS13* in two varieties was verified for accuracy and reliability (Fig. 6-A).

3.7. Subcellular localization of OfGGPPS13

In the control group, the GFP::pSuper1300 fusion protein auto-fluoresced green, while the chloroplasts in the cells auto-fluoresced red. The green and red fluorescence did not merge in the merged layer. The GFP fluorescence signal of the GFP::pSuper1300-OfGGPPS13 fusion protein coincided with chloroplast auto-fluorescence (Fig. 6-B), indicating that the OfGGPPS13 protein was localized in chloroplasts, which is consistent with subcellular prediction results.

3.8. Functional validation of *OfGGPPS13* transgenic petals

To further reveal the potential functions of *OfGGPPS13* in regulating the formation of floral color and fragrance in the MEP pathway, *OfGGPPS13* was transiently expressed in *O. fragrans* petals. The qRT-PCR results showed that the expression level of *OfGGPPS13* was significantly increased in transgenic plants, which was twice that in the control (Fig. 7-A). The expression of *CCD4* and *TPSs* downstream of *GGPPSs* was significantly decreased compared with the control (Fig. 8-D, G and H). The content of each substance on the MEP pathway was determined, and there was a significant increase in the content of GGPPS, its direct product, GGPP, and the subsequent product of GGPP, *β*-carotene, after *OfGGPPS13* overexpression in *O. fragrans* petals (Fig. 8-A–C). On the other pathway competing with GGPPS for the substrates DMAPP and IPP, there was a significant decrease in the content of GPPS and GPP (Fig. 8-E

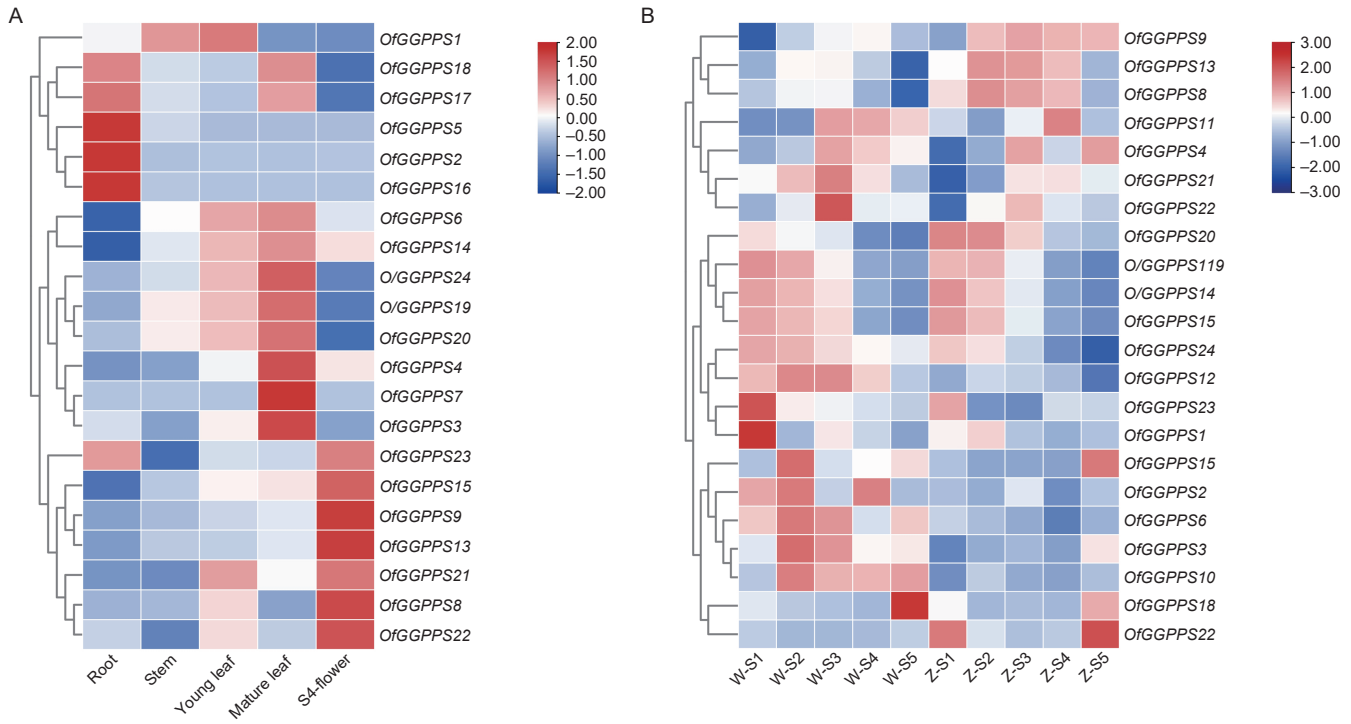


Fig. 5 Expression patterns of *OfGGPPSs* were analyzed. A, clusters of the expression levels of *OfGGPPSs* in 5 different tissues which were root, stem, young leaves, mature leaves, and S4 flowers. B, clusters of the expression levels of *OfGGPPSs* in 'Wanyingui' (W) and 'Zhuangyuanhong' (Z).

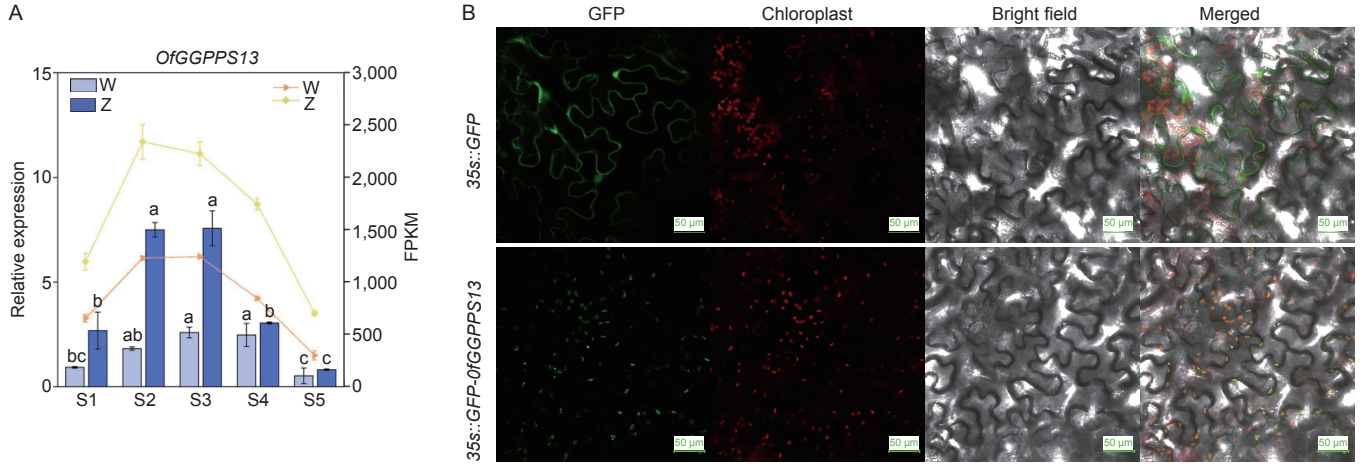
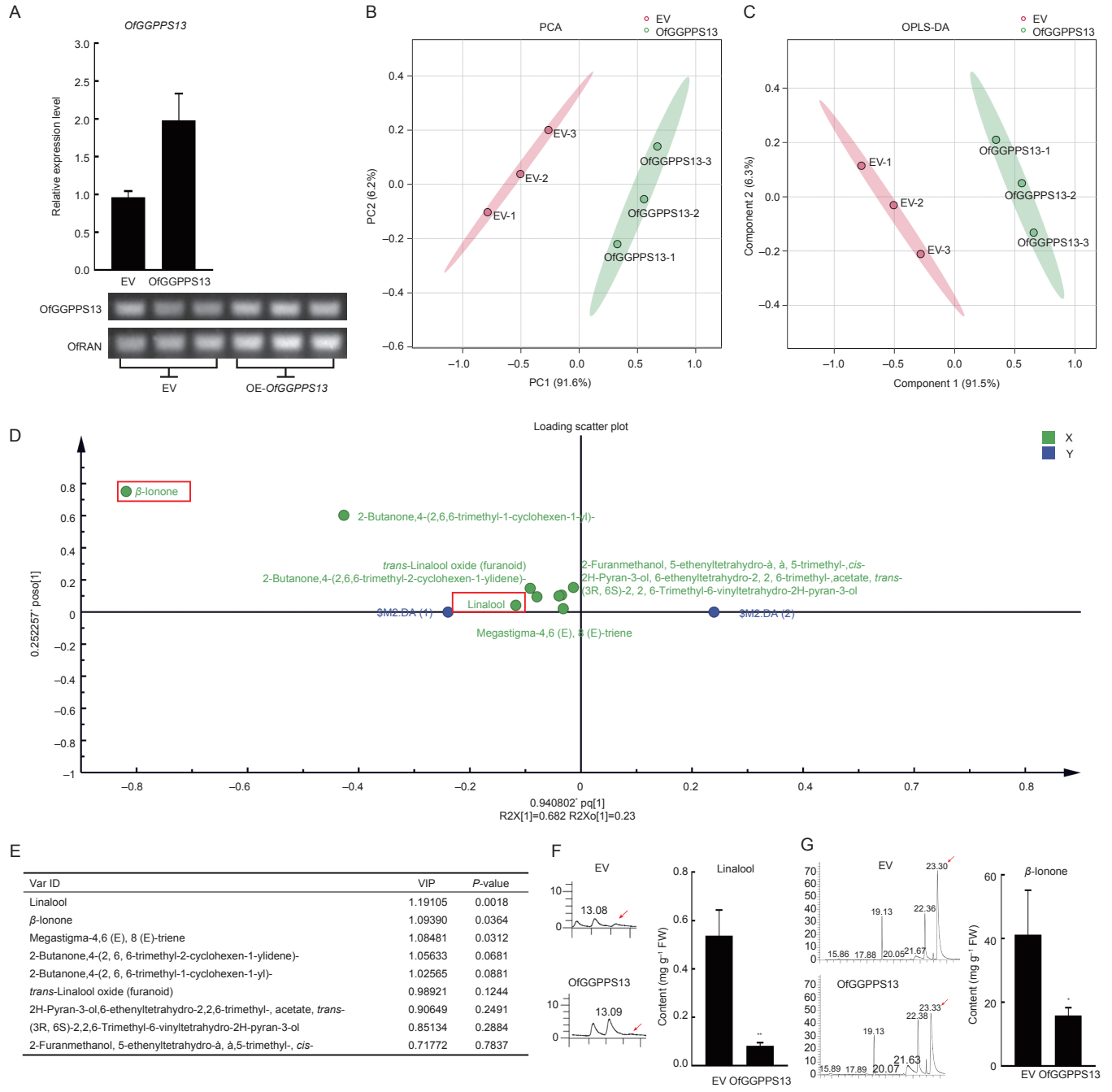


Fig. 6 Expression patterns and subcellular localization of *OfGGPPS13* were analyzed. A, expression pattern of *OfGGPPS13*. W, 'Wanyingui'; Z, 'Zhuangyuanhong'. Data are presented as the mean±SE (n=3). Different lowercase letters on the column indicate significant differences in the flowering period of the same variety (P<0.05) (two-tailed Student's t-test). B, subcellular localization map of OfGGPPS13.

and F), demonstrating that *OfGGPPS13* promoted the accumulation of *β*-carotene through the MEP pathway and was crucial for color formation in *O. fragrans* flowers. Based on GC-MS analysis, the PCA-X and PLS-DA plots showed that *OfGGPPS13*-overexpressing petals exhibited significant metabolic differences compared with the petals transformed with the empty vector (Fig. 7-B and C), and the loading scatter plot showed that linalool and *β*-ionone were the main substances that caused changes in aroma (Fig. 7-D and E). The *OfGGPPS13*-overexpressing petals had significantly lower contents of linalool and *β*-ionone (Fig. 7-F and G), demonstrating that *OfGGPPS13* was also crucial for aroma formation in *O. fragrans* flowers.

4. Discussion

GGPPSs catalyze GGPP synthesis, and GGPP is crucial for the isoprenoid pathway, providing common precursors for primary and secondary metabolism (Schmidt *et al.* 2010).



Var ID	VIP	*P*-value
Linalool	1.19105	0.0018
β-Ionone	1.09390	0.0364
Megastigma-4,6 (E), 8 (E)-triene	1.08481	0.0312
2-Butanone,4-(2, 6, 6-trimethyl-2-cyclohexen-1-ylidene)-	1.05633	0.0681
2-Butanone,4-(2, 6, 6-trimethyl-1-cyclohexen-1-yl)-	1.02565	0.0881
trans-Linalool oxide (furanoid)	0.98921	0.1244
2H-Pyran-3-ol,6-ethenyltetrahydro-2,2,6-trimethyl-, acetate, *trans*-	0.90649	0.2491
(3R, 6S)-2,2,6-Trimethyl-6-vinyltetrahydro-2H-pyran-3-ol	0.85134	0.2884
2-Furanmethanol, 5-ethenyltetrahydro-à, à,5-trimethyl-, *cis*-	0.71772	0.7837

Fig. 7 Volatile organic compounds (VOCs) of *OfGGPPS13* transgenic petals were analyzed. A, semi-quantitative and fluorescence quantitative results of transgenic *OfGGPPS13* petals. The transcript level of EV was set to 1. Data are presented as the mean±SE (*n*=3). *, *P*<0.05 (two-tailed Student's *t*-test). B, PLS-DA analysis of VOCs in transgenic *OfGGPPS13* petals. C, PCA analysis of VOCs in transgenic *OfGGPPS13* petals. D, compositional map of VOCs in transgenic *OfGGPPS13* petals. E, VIP and *P*-value of VOCs in transgenic *OfGGPPS13* petals. F, linalool content in transgenic *OfGGPPS13* petals. Data are presented as the mean±SE (*n*=3). **, *P*<0.01 (two-tailed Student's *t*-test). G, *β*-ionone content in transgenic *OfGGPPS13* petals. Data are presented as the mean±SE (*n*=3). *, *P*<0.05 (two-tailed Student's *t*-test).

In this study, 24 *OfGGPPSs* were identified (Fig. 2-A), with a much larger number than in *A. thaliana* (12) (Lange and Ghassemian 2003) and *N. tabacum* (9) (Tata *et al.* 2016) but comparable to the 25 in the *G. hirsutum* GGPPS gene family (Ali *et al.* 2020). The differences in the number of *GGPPSs* between species may result from evolutionary differences. The 24 OfGGPPSs were classified into sub4 and sub5 subfamilies (Fig. 1). Analysis of the protein structure of OfGGPPSs revealed that the same subfamily contained similar domains, and the OfGGPPS proteins of different subfamilies differed in structure (Fig. 3).

The OfGGPPS proteins contained two conserved Asp-rich structural domains, FARM and SARM (Fig. 4), with a conserved sequence of "DDxx(xx)D", which were crucial for the catalytic activity of GGPPS (Liang *et al.* 2002; Liang 2009). The "CxxxC" motif was also found in OfGGPPSs.

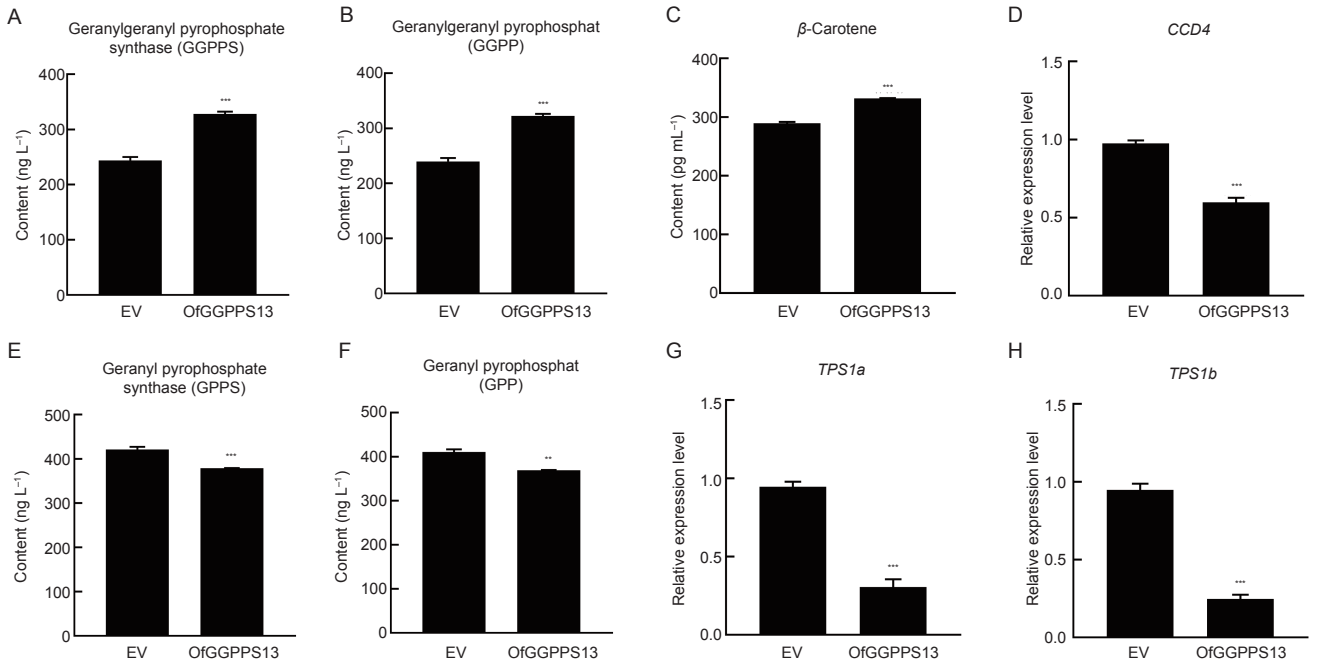


Fig. 8 Contents of key substances and expression levels of key genes in EV and OE-*OfGGPPS13*. A, GGPPS content. B, GGPP content. C, *β*-carotene content. D, expression level of *CCD4*. E, GGPS content. F, GGP content. G, expression level of *TPS1a*. H, expression level of *TPS1b*. Data are presented as the mean±SE (n=3). **, P<0.01; ***, P<0.001 (two-tailed Student's t-test).

The "CxxxC" domain is important for GGPPSs to interact with other proteins, but some GGPPSs with "CxxxC" are non-functional (Zhang *et al.* 2021). Proteins characterized by FARM, SARM, and "CxxxC" exhibit the catalytic function for the GGPP formation (Beck *et al.* 2013), indicating that some *OfGGPPSs*, such as *OfGGPPS9/13/20*, may be employed in similar functions.

GGPPSs exist as a gene family in higher plants, and there are many members. Since the emergence of land plants, gene duplication has led to the expression pattern changes of GGPPS paralogs, leading to developmental and/or condition-specific functional evolution (Coman *et al.* 2014). Therefore, it can provide a foundation for gene function research to characterize the expression patterns and subcellular localization of *GGPPSs* (Ruiz-Sola *et al.* 2016). The synthesis of GGPP in different subcellular structures is handled by different members, but it has been shown that *AtGGPPS*s are predominantly localized to chloroplasts (Zhu *et al.* 1997a, b; Okada *et al.* 2000).

In a previous study, *AtGGPPSs* were found to have different expression levels in tissues and organs throughout the growth and development of *A. thaliana* and have different functions in the plant (Okada *et al.* 2000; Beck *et al.* 2013). In sweetpotato (*Ipomoea batatas* (L.) Lam.), the expression levels of *IbGGPPSs* were high in storage roots but low in stems and leaves, and the storage roots had antioxidative activity due to the high production of carotenoids (Chen W *et al.* 2015). The transcriptome data showed that the *OfGGPPSs* were expressed in different tissues and organs of *O. fragrans* (Fig. 5-A). We speculated that *OfGGPPSs* may play different roles in different parts of the plant due to tissue-specific expression. *OfGGPPS2/5/16* had higher expression levels in roots, which may be related to root growth and development. Nine genes, including *OfGGPPS3/7*, were more highly expressed in mature leaves, which might be involved in chlorophyll synthesis in mature leaves. *OfGGPPS8/9/13/15/21/22* had the highest expression in flowers, which may participate in the regulation of flower growth. A few *OfGGPPSs* had low transcription levels and almost no expression abundance at each developmental stage, inferring that they may perform minor functions in different *O. fragrans* tissues.

In a previous study, the expression patterns of *RdGGPPSs* were consistent with the contents of aroma compounds in *R. damascena* flowers (Rasouli *et al.* 2018). Differences in the expression of *OfGGPPSs* were found in 'Wanyinggui' and 'Zhuangyuanhong' using the expression pattern analysis (Fig. 5-B). The expression of most of the *OfGGPPSs* tended to increase at first and then decrease in the flower development stages of 'Wanyinggui' and 'Zhuangyuanhong', which was consistent with the release pattern of fragrance in flowers.

In this study, we found OfGGPPS13 protein contained DDxxxxD and DDxxD, which are essential for GGPP (the precursor of *β*-carotene) biosynthesis. The expression level of *OfGGPPS13* was the highest in 'Zhuangyuanhong' and significantly higher than that in 'Wanyingui' (Fig. 5-B). Moreover, it had its highest expression level in the flowers (Fig. 5-A) and its expression agreed with the release pattern of fragrance (Fig. 5-B) in flowers. We speculated that *OfGGPPS13* is a key candidate gene in the floral aroma and color formation. The qRT-PCR method was used to verify the transcriptome data of *OfGGPPS13* in two *O. fragrans* cultivars 'Wanyingui' and 'Zhuangyuanhong' at different

flower development stages. The results were correlated with the transcriptome FPKM values (Fig. 6-A). It has been reported that the differential expression of *GGPPSs* between the two *Syringa* varieties led to differences in floral content (Yang *et al.* 2023). 'Wanyingui' has a strong fragrance but lighter color, while 'Zhuangyuanhong' has a lighter fragrance but a strong color. According to the relative expression of the *OfGGPPS13* gene in the two varieties, expression in 'Zhuangyuanhong' was significantly higher than that in 'Wanyingui'. It was presumed that *OfGGPPS13* was the key gene responsible for the difference in color and aroma in *O. fragrans* flowers. Carotenoids are synthesized in plant plastids (Sun *et al.* 2018). The OfGGPPS13 protein was located in the chloroplast (Fig. 6-B), indicating that *OfGGPPS13* may be related to carotenoid biosynthesis and may further affect the formation of floral color.

GGPPSs can promote carotenoid biosynthesis. There is a positive linear relationship between GGPPS enzyme activity and the *β*-carotene synthesis content in different *Dunaliella* species (Xu *et al.* 2021). Original overexpression of *IbGGPS* was found to increase the carotenoid content in transgenic plants and may potentially increase the carotenoid content in other plants (Chen W *et al.* 2015). After overexpression of *OfGGPPS13*, there was a significant increase in the contents of GGPPS (Fig. 8-A) and its direct product GGPP (Fig. 8-B) in petals. The content of *β*-carotene (Fig. 8-C), the subsequent product of GGPP, also increased significantly. However, the content of GPPS (Fig. 8-E) decreased significantly in another pathway competing with GGPPS for substrates DMAPP and IPP. The content of GPP (Fig. 8-F), the direct product of GPPS and the precursor of linalool, also showed a significant decrease. GC-MS analysis showed that the linalool content (Fig. 7-F) in the *OfGGPPS13* transgenic petals was significantly decreased compared with the petals transformed by the empty vector, which was consistent with the decrease in the expression of *TPS1a* (Fig. 8-G), *TPS1b* (Fig. 8-H), the genes downstream of the *GGPPS* genes. Terpene synthases (TPSs) are the key rate-limiting enzymes that catalyze the monoterpene formation, such as linalool, from GPP in the final step (Dudareva *et al.* 2013). The proteins encoded by *CCD4* genes can cleave *β*-carotene to *β*-ionone (Huang *et al.* 2009). Interestingly, we found that the expression of *CCD4* (Fig. 8-D) and the content of *β*-ionone (Fig. 7-G) were significantly decreased when the content of *β*-carotene increased significantly in the *OfGGPPS13* transgenic petals in this study. The regulatory mechanisms involved require further study. Overall, the *OfGGPPS13* gene promoted the accumulation of *β*-carotene and decreased the contents of linalool and *β*-ionone. By regulating *OfGGPPS13*, it may be possible to simultaneously regulate the production of the products of the two pathways, changing the direction of metabolic flux between the biosynthesis pathways of monoterpenes and carotenoids and thus affecting floral color and aroma formation.

5. Conclusion

In this study, 24 members of the GGPPS gene family in *O. fragrans* were identified and characterized. The transcriptome data suggested that *OfGGPPSs* expressed in different tissues with specificity. Among them, *OfGGPPS13* had a higher expression level in 'Zhuangyuanhong' compared with 'Wanyingui', and the expression showed a tendency of increasing and then decreasing at the five flowering stages which consistent with the release pattern of fragrance in flowers. After overexpression of *OfGGPPS13* in *O. fragrans* petals, the contents of GGPPS, GGPP and *β*-carotene were significantly increased and the linalool content in the aromatic constituents was significantly decreased, demonstrating that *OfGGPPS13* influenced monoterpene biosynthesis and promoted *β*-carotene accumulation. Above all, we found *OfGGPPS13* can simultaneously affect the floral color and fragrance, revealing the regulatory mechanism of floral color and fragrance in *O. fragrans*.

Acknowledgements

This research was funded by the National Natural Science Foundation of China (32071828 and 32471943), the Central Finance Forestry Science and Technology Promotion Demonstration Project, China (Su2024TG04), the Priority Academic Program Development of Jiangsu Higher Education Institutions (PAPD), China, and partly supported by the open funds of the National Key Laboratory for Germplasm Innovation & Utilization of Horticultural Crops, China.

Declaration of competing interest

The authors declare that they have no conflict of interest.

Declaration of generative AI and AI-assisted technologies in the writing process

The authors declare that they did not use AI in the preparation and writing of this manuscript.

Appendices associated with this paper are available at https://doi.org/10.1016/j.jia.2025.11.029

References

Ali F, Qanmber G, Wei Z, Yu D, Li Y H, Gan L, Li F, Wang Z. 2020. Genome-wide characterization and expression analysis of geranylgeranyl diphosphate synthase genes in cotton (*Gossypium* spp.) in plant development and abiotic stresses. *BMC Genomics*, **21**, 561.

Barja M V, Rodriguez-Concepcion M. 2021. Plant geranylgeranyl diphosphate synthases: Every (gene) family has a story. *aBiotech*, **2**, 289–298.

Beck G, Coman D, Herren E, Ruiz-Sola M A, Rodriguez-Concepcion M, Gruissem W, Vranova E. 2013. Characterization of the GGPP synthase gene family in *Arabidopsis thaliana*. *Plant Molecular Biology*, **82**, 393–416.

Bouvier F, Suire C, D'Harlingue A, Backhaus R A, Camara B. 2000. Molecular cloning of geranyl diphosphate synthase and compartmentation of monoterpene synthesis in plant cells. *Plant Journal*, **24**, 241–252.

Cai X, Mai R, Zou J, Zhang H, Zeng X, Zheng R, Wang C. 2014. Analysis of aroma-active compounds in three sweet osmanthus (*Osmanthus fragrans*) cultivars by GC-olfactometry and GC-MS. *Journal of Zhejiang University — Science B*, **15**, 638–648.

Chen Q, Fan D, Wang G. 2015. Heteromeric geranyl(geranyl) diphosphate synthase is involved in monoterpene biosynthesis in *Arabidopsis* flowers. *Molecular Plant*, **8**, 1434–1437.

Chen W, He S, Liu D, Patil G B, Zhai H, Wang F, Stephenson T J, Wang Y, Wang B, Valliyodan B, Nguyen H T, Liu Q. 2015. A sweetpotato geranylgeranyl pyrophosphate synthase gene, *IbGGPS*, increases carotenoid content and enhances osmotic stress tolerance in

Arabidopsis thaliana. *PLoS ONE*, **10**, e137623.
Coman D, Altenhoff A, Zoller S, Gruissem W, Vranova E. 2014. Distinct evolutionary strategies in the GGPPS family from plants. *Frontiers in Plant Science*, **5**, 230.
Ding W, Ouyang Q, Li Y, Shi T, Li L, Yang X, Ji K, Wang L, Yue Y. 2020. Genome-wide investigation of WRKY transcription factors in sweet osmanthus and their potential regulation of aroma synthesis. *Tree Physiology*, **40**, 557–572.
Dong C, Qu G, Guo J, Wei F, Gao S, Sun Z, Jin L, Sun X, Rochaix J D, Miao Y, Wang R. 2022. Rational design of geranylgeranyl diphosphate synthase enhances carotenoid production and improves photosynthetic efficiency in *Nicotiana tabacum*. *Science Bulletin*, **67**, 315–327.
Dudareva N, Klempien A, Muhlemann J K, Kaplan I. 2013. Biosynthesis, function and metabolic engineering of plant volatile organic compounds. *New Phytologist*, **198**, 16–32.
Han Y, Wu M, Cao L, Yuan W, Dong M, Wang X, Chen W, Shang F. 2016. Characterization of OfWRKY3, a transcription factor that positively regulates the carotenoid cleavage dioxygenase gene *OfCCD4* in *Osmanthus fragrans*. *Plant Molecular Biology*, **91**, 485–496.
Huang D, Liu W, Li A, Wang C, Hu Z. 2019. Discovery of geranylgeranyl pyrophosphate synthase (GGPPS) paralogs from *Haematococcus pluvialis* based on Iso-seq analysis and their function on astaxanthin biosynthesis. *Marine Drugs*, **17**, 696.
Huang F C, Molnar P, Schwab W. 2009. Cloning and functional characterization of carotenoid cleavage dioxygenase 4 genes. *Journal of Experimental Botany*, **60**, 3011–3022.
Ji X. 2021. Comparative investigation of volatile components and bioactive compounds in beers by multivariate analysis. *Flavour and Fragrance Journal*, **36**, 374–383.
Lange B M, Ghassemian M. 2003. Genome organization in *Arabidopsis thaliana*: A survey for genes involved in isoprenoid and chlorophyll metabolism. *Plant Molecular Biology*, **51**, 925–948.
Liang P. 2009. Reaction kinetics, catalytic mechanisms, conformational changes, and inhibitor design for prenyltransferases. *Biochemistry*, **48**, 6562–6570.
Liang P H, Ko T P, Wang A. 2002. Structure , mechanism and function of prenyltransferases. *European Journal of Biochemistry*, **269**, 3339–3354.
Liu J, Hu H, Shen H, Tian Q, Ding W, Yang X, Wang L, Yue Y. 2022. Insights into the cytochrome P450 monooxygenase superfamily in *Osmanthus fragrans* and the role of *OfCYP142* in linalool synthesis. *International Journal of Molecular Sciences*, **23**, 12150.
Lois L M, Rodriguez-Concepcion M, Gallego F, Campos N, Boronat A. 2000. Carotenoid biosynthesis during tomato fruit development: Regulatory role of 1-deoxy-d-xylulose 5-phosphate synthase. *Plant Journal*, **22**, 503–513.
Matthews P D, Wurtzel E T. 2000. Metabolic engineering of carotenoid accumulation in *Escherichia coli* by modulation of the isoprenoid precursor pool with expression of deoxyxylulose phosphate synthase. *Applied Microbiology and Biotechnology*, **53**, 396–400.
Mcgarvey D J, Croteau R. 1995. Terpenoid metabolism. *Plant Cell*, **7**, 1015–1026.
Newman J D, Chappell J. 1999. Isoprenoid biosynthesis in plants: Carbon partitioning within the cytoplasmic pathway. *Critical Reviews in Biochemistry and Molecular Biology*, **34**, 95–106.
Okada K, Saito T, Nakagawa T, Kawamukai M, Kamiya Y. 2000. Five geranylgeranyl diphosphate synthases expressed in different organs are localized into three subcellular compartments in *Arabidopsis*. *Plant Physiology*, **122**, 1045–1056.
Orlova I, Nagegowda D A, Kish C M, Gutensohn M, Maeda H, Varbanova M, Fridman E, Yamaguchi S, Hanada A, Kamiya Y, Krichevsky A, Citovsky V, Pichersky E, Dudareva N. 2009. The small subunit of snapdragon geranyl diphosphate synthase modifies the chain length specificity of tobacco geranylgeranyl diphosphate synthase in planta. *Plant Cell*, **21**, 4002–4017.
Pichersky E, Gershenzon J. 2002. The formation and function of plant volatiles: Perfumes for pollinator attraction and defense. *Current Opinion in Plant Biology*, **5**, 237–243.
Rasouli O, Ahmadi N, Monfared S R, Sefidkon F. 2018. Physiological, phytochemicals and molecular analysis of color and scent of different landraces of *Rosa damascena* during flower development stages. *Scientia Horticulturae*, **231**, 144–150.
Ruiz-Sola M A, Coman D, Beck G, Barja M V, Colinas M, Graf A, Welsch R, Rutimann P, Buhlmann P, Bigler L, Gruissem W, Rodriguez-Concepcion M, Vranova E. 2016. *Arabidopsis* GERANYLGERANYL DIPHOSPHATE SYNTHASE 11 is a hub isozyme required for the production of most photosynthesis-related isoprenoids. *New Phytologist*, **209**, 252–264.
Satta A, Esquirol L, Ebert B E, Newman J, Peat T S, Plan M, Schenk G, Vickers C E. 2022. Molecular characterization of cyanobacterial short-chain prenyltransferases and discovery of a novel GGPP phosphatase. *FEBS Journal*, **289**, 6672–6693.
Schmidt A, Wachtler B, Temp U, Krekling T, Seguin A, Gershenzon J. 2010. A bifunctional geranyl and geranylgeranyl diphosphate synthase is involved in terpene oleoresin formation in *Picea abies*. *Plant Physiology*, **152**, 639–655.
Simkin A J, Guirimand G, Papon N, Courdavault V, Thabet I, Ginis O, Bouzid S, Giglioli-Guivarc'H N, Clastre M. 2011. Peroxisomal localisation of the final steps of the mevalonic acid pathway in planta. *Planta*, **234**, 903–914.
Sun T, Yuan H, Cao H, Yazdani M, Tadmor Y, Li L. 2018. Carotenoid metabolism in plants: The role of plastids. *Molecular Plant*, **11**, 58–74.
Tata S K, Jung J, Kim Y, Choi J Y, Jung J, Lee I, Shin J S, Ryu S B. 2016. Heterologous expression of chloroplast-localized geranylgeranyl pyrophosphate synthase confers fast plant growth, early flowering and increased seed yield. *Plant Biotechnology Journal*, **14**, 29–39.
Tholl D, Kish C M, Orlova I, Sherman D, Gershenzon J, Pichersky E, Dudareva N. 2004. Formation of monoterpenes in *Antirrhinum majus* and *Clarkia breweri* flowers involves heterodimeric geranyl diphosphate synthases. *Plant Cell*, **16**, 977–992.
Vranova E, Hirsch-Hoffmann M, Gruissem W. 2011. AtIPD: A curated database of arabidopsis isoprenoid pathway models and genes for isoprenoid network analysis. *Plant Physiology*, **156**, 1655–1660.
Wang G, Dixon R A. 2009. Heterodimeric geranyl(geranyl) diphosphate synthase from hop (*Humulus lupulus*) and the evolution of monoterpene biosynthesis. *Proceedings of the National Academy of Sciences of the United States of America*, **106**, 9914–9919.
Xu L, Gao F, Feng J, Lv J, Liu Q, Nan F, Liu X, Xie S. 2021. Relationship between beta-carotene accumulation and geranylgeranyl pyrophosphate synthase in different species of *Dunaliella*. *Plants-Basel*, **11**, 27.
Yan L, Fang Z, Zhang N, Yang L, Zhang Y, Zhuang M, Lv H, Ji J, Wang Y. 2023. Genome-wide identification, characterization, and expression analysis of the geranylgeranyl pyrophosphate synthase (GGPPS) gene family reveals its importance in chloroplasts of *Brassica oleracea* L. *Agriculture-Basel*, **13**, 1615.
Yang X, Yue Y, Li H, Ding W, Chen G, Shi T, Chen J, Park M S, Chen F, Wang L. 2019. The chromosome-level quality genome provides insights into the evolution of the biosynthesis genes for aroma compounds of *Osmanthus fragrans*. *Horticulture Research*, **1**, 102–114.
Yang Z, Zhu Y, Zhang X, Zhang H, Zhang X, Liu G, Zhao Q, Bao Z, Ma F. 2023. Volatile secondary metabolome and transcriptome analysis reveals distinct regulation mechanism of aroma biosynthesis in *Syringa oblata* and *S. vulgaris*. *Plant Physiology and Biochemistry*, **196**, 965–973.
Zhang C, Liu H, Zong Y, Tu Z, Li H. 2021. Isolation, expression, and functional analysis of the geranylgeranyl pyrophosphate synthase (GGPPS) gene from *Liriodendron tulipifera*. *Plant Physiology and Biochemistry*, **166**, 700–711.
Zhu X F, Suzuki K, Okada K, Tanaka K, Nakagawa T, Kawamukai M, Matsuda K. 1997a. Cloning and functional expression of a novel geranylgeranyl pyrophosphate synthase gene from *Arabidopsis thaliana* in *Escherichia coli*. *Plant and Cell Physiology*, **38**, 357–361.
Zhu X F, Suzuki K, Saito T, Okada K, Tanaka K, Nakagawa T, Matsuda H, Kawamukai M. 1997b. Geranylgeranyl pyrophosphate synthase encoded by the newly isolated gene *GGPS6* from *Arabidopsis thaliana* is localized in mitochondria. *Plant Molecular Biology*, **35**, 331–341.

Executive Editor-in-Chief Sanwen Huang
Managing Editor Lingyun Weng